Article

Preclinical Studies of the Potent and Selective Nicotinic α4β2 Receptor Ligand VMY-2-95

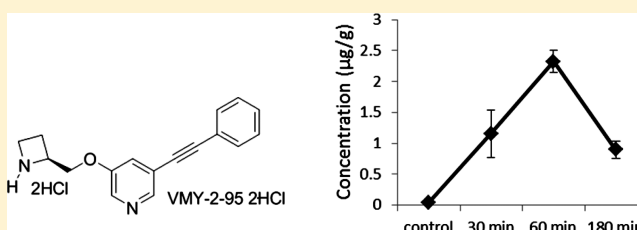Hyesik Kong,[†,‡,⊥] Jun-ke Song,[‖,⊥] Venkata Mahidhar Yenugonda,[†,‡] Li Zhang,[†,‡] Tian Shuo,[‖] Amrita K. Cheema,[†,§] Yali Kong,[†,‡] Guan-hua Du,[‖] and Milton L. Brown*,[†,‡]

[†]Department of Oncology, [‡]Center for Drug Discovery, and [§]Lombardi Comprehensive Cancer Center, Georgetown University Medical Center, 3970 Reservoir Road, Washington D.C. 20057, United States

[‖]Institute of Materia Medica, Chinese Academy of Medical Sciences and Peking Union Medical College, 1 Xian Nong Tan Street, Beijing 100050, China

Ⓢ Supporting Information

ABSTRACT: The discovery and development of small molecules that antagonize neuronal nicotinic acetylcholine receptors may provide new ligands for evaluation in models of depression or addiction. We discovered a small molecule, VMY-2-95, a nAChR ligand with picomolar affinity and high selectivity for α4β2 receptors. In this study, we investigated its preclinical profile in regards to solubility, lipophilicity, metabolic stability, intestinal permeability, bioavailability, and drug delivery to the rat brain. Metabolic stability of VMY-2-95·2HCl was monitored on human liver microsomes, and specific activity of VMY-2-95·2HCl on substrate metabolism by CYP1A2, 2C9, 2C19, 2D6, and 3A4 was tested in a high-throughput manner. The intestinal transport of VMY-2-95·2HCl was studied through Caco-2 cell monolayer permeability. VMY-2-95·2HCl was soluble in water and chemically stable, and the apparent partition coefficient was 0.682. VMY-2-95·2HCl showed significant inhibition of CYP2C9 and 2C19, but weak or no effect on 1A2, 2D6, and 3A4. The Caco-2 cell model studies revealed that VMY-2-95·2HCl was highly permeable with efflux ratio of 1.11. VMY-2-95·2HCl achieved a maximum serum concentration of 0.56 mg/mL at 0.9 h and was orally available with a half-life of ~9 h. Furthermore, VMY-2-95·2HCl was detected in the rat brain after 3 mg/kg oral administration and achieved a maximal brain tissue concentration of 2.3 μg/g within 60 min. Overall, the results demonstrate that VMY-2-95·2HCl has good drug like properties and can penetrate the blood−brain barrier with oral administration.

KEYWORDS: preclinical metabolism, VMY-2-95, α4β2 nicotinic receptor ligand, drug delivery

INTRODUCTION

Nicotine addiction is responsible for about one in five deaths annually contributing to over 443,000 deaths per year in the United States. The impact of cigarette smoking on increased healthcare cost is enormous resulting in more than $193 billion dollars per year.[1] These facts emphasize the need to develop new therapeutics that effectively help patients decrease or eliminate nicotine addiction.

There are at least 17 nicotinic acetylcholine receptor (nAChR) subtypes, and the combination of protein subunits can generate a large number of functional pentameric channels.[2,3] The human α2−α7 and β2−β4 subunits have been cloned and found to be localized in specific tissues (ganglion-type (α3)2(β4)3 versus CNS-type (α4)2(β2)3 (CNS-type)). Several of these subtypes have been linked to suppression of nicotine mediated addiction[4−8] and the development of small molecules that modulate them selectively may lead to discovery of new channel physiology and/or pharmacology.

Compounds that modulate nAChR can be classified as agonists, partial agonists, or antagonists. Depending on

concentration and time of exposure, compounds that mitigate acetylcholine (ACh) mediated pathways can have potentially important pharmacological functions. Compounds that function as antagonists of the nAChR inhibit the action of ACh at nicotinic acetylcholine receptors. Chronic exposure to agonist can also lead to long lasting functional deactivation because of rapid and persistent desensitization.

Small molecule ligands can act as subtype selective partial agonists for one type of nAChRs and an antagonist of another subtype. For example, a compound can act as an agonist at (α4)2(β2)3 pentamers, but as an antagonist at (α4)3(β2)2 pentamers. Thus, the discovery of subtype and state selective nAChR ligands will help in understanding important receptor pharmacology and developing new therapeutic interventions.

We previously reported[9] the synthesis and pharmacological properties of VMY-2-95, a potent and selective inhibitor of
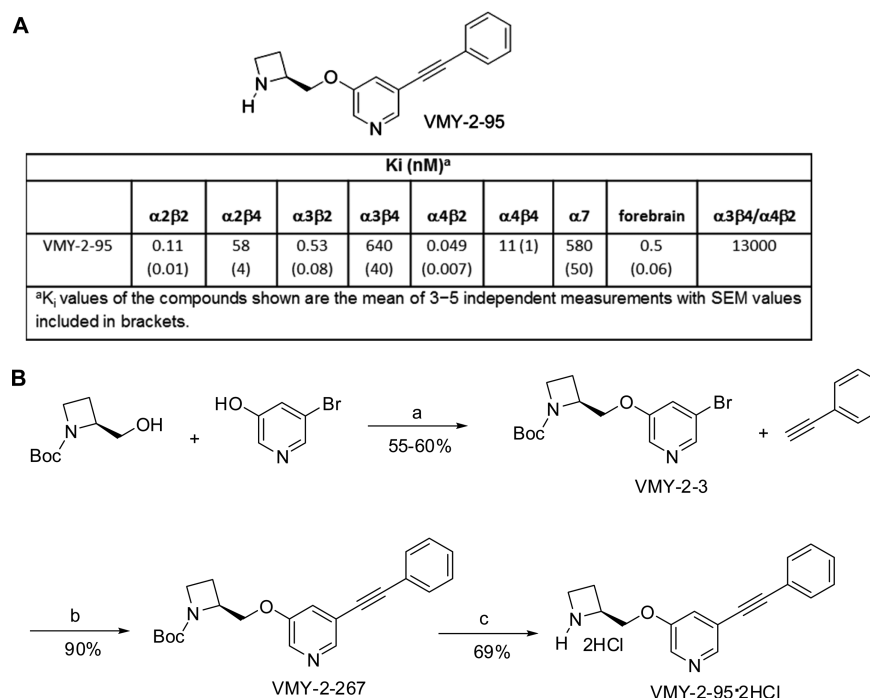
Figure 1. (A) Chemical structure of VMY-2-95. (B) Synthesis of VMY-2-95·2HCl: a, DEAD, PPh$_3$, THF, 0 °C, 48 h; b, 4 mol % Pd(PPh$_3$)$_2$Cl$_2$, 8 mol % PPh$_3$, 8 mol % CuI, iPr$_2$NH, toluene, 80 °C, 18 h; c, 1.25 M HCl in MeOH, rt, overnight.

$\alpha 4\beta 2$ nAChR. VMY-2-95 potently inhibits the $\alpha 4\beta 2$ nAChR with an IC$_{50}$ of 0.049 nM. The inhibition was selective (2 to 13,000 times) for the $\alpha 4\beta 2$ subtype as compared to other nicotinic receptor subtypes ($\alpha 2\beta 2$, $\alpha 2\beta 4$, $\alpha 3\beta 2$, $\alpha 3\beta 4$, $\alpha 4\beta 2$, $\alpha 4\beta 4$, and $\alpha 7$). A subcutaneous dose of 3 mg/kg of free base VMY-2-95 was effective at reducing nicotine self-administration in rats.[9] With this in mind, we investigated VMY-2-95 for its preclinical profile in regards to solubility, lipophilicity, metabolic stability, intestinal permeability, and oral bioavailability.

MATERIALS AND METHODS

Materials. 1-Octanol, hydrogen peroxide, magnesium chloride, acetic acid, phosphoric acid, triethylamine, propranolol, atenolol, dimethyl sulfoxide (DMSO), D-glucose 6-phosphate sodium salt, nonessential amino acids (NEAA), glucose-6-phosphate dehydrogenase (G-6-PDH), β-nicotinamide adenine dinucleotide phosphate sodium salt (NADP$^+$), verapamil, MK-571, testosterone, sodium phosphate monobasic monohydrate, sodium phosphate dibasic, Pd(PPh$_3$)$_2$Cl$_2$, CuI, PPh$_3$, i-Pr$_2$NH, toluene, and ethynylbenzene were purchased from Sigma (St. Louis, MO). Sodium pyruvate, Hank's Balanced Salt Solution (HBSS), and Phosphate-Buffered Saline (PBS) were from Cellgro (Manassas, VA). Hepes, glutamine, fetal bovine serum (FBS), and penicillin/streptomycin were from Invitrogen (St. Louis, MO). NaCl, NH$_4$Cl, CH$_2$Cl$_2$, sodium sulfate, formalin, hydrochloric acid, paraffin phosphate buffer, HPLC grade-acetonitrile, ethyl acetate, ethanol, and methanol were from Fisher Scienftic Co. (Pittsburgh, PA). Polyethylene glycol 400 (PEG) was from Hampton (Aliso Viejo, CA).

Preparation of VMY-2-95. We prepared VMY-2-95 as described in the reported method.[9]

Preparation of VMY-2-95·2HCl. The VMY-2-95·2HCl was prepared as shown in Figure 1. The Mitsunobu adduct

(VMY-2-3, 0.770 g, 2.24 mmol), Pd(PPh$_3$)$_2$Cl$_2$ (0.063 g, 0.09 mmol, 4 mol %), CuI (0.017 g, 8 mol %), and PPh$_3$ (0.047 g, 8 mol %) were placed in an oven-dried round-bottom flask under nitrogen atmosphere. After addition of i-Pr$_2$NH (1 mL) and toluene (3–5 mL), the mixture was stirred at room temperature for 10 min and ethynylbenzene (0.618 g, 6.05 mmol) was added and stirred at room temperature for another 10 min. The whole reaction mixture was stirred at 80 °C for 18 h. The reaction mixture was quenched with saturated NH$_4$Cl solution and extracted with CH$_2$Cl$_2$. The combined organic layers were washed with 2 N HCl, water, and saturated NaCl solution. The organic phase was separated and dried over anhydrous sodium sulfate, filtered, and concentrated under reduced pressure. The crude product (TLC: R_f = 0.4, 40% EtOAc/hexane) was purified on a Biotage SNAP flash cartridge (40 g, KP-SIL) using methanol–CH$_2$Cl$_2$ (2–4%) as the eluent to afford 0.740 g of VMY-2-267 (90% yield). HRMS (ESI) m/z calcd for C$_{22}$H$_{24}$N$_2$O$_3$ (M + H)$^+$ 365.1865, found 365.1879. ^{1}H NMR (400 MHz, CDCl$_3$) δ 8.31 (s, 1H), 8.22 (s, 1H), 7.51–7.42 (m, 2H), 7.34–7.26 (m, 4H), 4.52–4.40 (m, 1H), 4.28 (s, 1H), 4.12–4.06 (m, 1H), 3.82 (t, J = 7.6, 2H), 2.36–2.15 (m, 2H), 1.36 (s, 9H). ^{13}C NMR (100 MHz, CDCl$_3$) δ 156.13, 154.49, 144.77, 137.89, 131.66, 128.78, 128.41, 123.00, 122.46, 120.60, 92.44, 85.78, 79.77, 68.73, 60.04, 47.09, 28.41, 19.08. HCl (1.25 M) in methanol (11 mL, 13.2 mmol) was slowly added to the boc-protected compound VMY-2-267 (0.240 g, 0.66 mmol) at 0 °C under a nitrogen atmosphere. The reaction mixture was allowed to warm at room temperature and stirred for overnight. The reaction mixture was concentrated under reduced pressure, and the residue (TLC: R_f = 0.3, 20% methanol–CH$_2$Cl$_2$) was purified on a Biotage SNAP flash cartridge (25 g, KP-SIL), using methanol–CH$_2$Cl$_2$ (12–14%) as the eluent, to afford the product as light yellow solid (mp = 137.1 °C) in 69% yield. HRMS (ESI) m/z calcd for C$_{17}$H$_{16}$N$_2$O·2HCl (M + H)$^+$ 265.1341(−2HCl), found 265.1344. Anal. Calcd for C$_{17}$H$_{16}$N$_2$O·2HCl·2.5H$_2$O: C,

53.69; H, 5.56; N, 7.36; Cl, 18.64. Found: C, 53.70; H, 5.82; N, 7.29, Cl, 18.25. ^{1}H NMR (400 MHz, D_2O) δ 8.47 (brs, 1H), 8.41 (brs, 1H), 8.16 (brs, 1H), 7.57−7.50 (m, 2H), 7.45−7.33 (m, 3H), 4.92 (tt,1H), 4.45 (brs, 2H), 4.04 (m, 2H), 2.63 (q, 2H), see Supporting Information Figure 3. ^{13}C NMR (100 MHz, CD_3OD) δ 156.54, 137.09, 132.65, 131.68, 129.95, 128.48, 124.72, 120.82,96.56, 81.77, 68.32, 58.66, 43.43, 20.34, see Supporting Information Figure 4.

Cell Culture. Caco-2 cells were purchased from the Tissue Culture Shared Resources of the Lombardi Comprehensive Cancer Center in Georgetown University (Washington, DC). The cells were cultured in DMEM. The medium was supplemented with 10% FBS, glutamine, Hepes, sodium pyruvate, penicillin/streptomycin, and NEAA. A 24-well BIOCOAT HTS Fibrillar Collagen Multiwell Insert System was obtained from BD Biosciences (Bedford, MA) for Caco-2 cell monolayer transport study. Caco-2 cells were seeded at a density of 6×10^5 cells/cm^2 on a 24-well system, cultured in the seeding medium by following the manufacturer's instructions, and using the method of Uchida et al.[24] After incubation for 24 h, the medium was replaced with the cell differentiation-inducing medium, which was provided with BIOCOAT HTS Fibrillar Collagen Multiwell Insert System and incubated for 72 h.

Caco-2 Cell Permeability Studies. The transport studies were performed by using BIOCOAT HTS Caco-2 Assay System (BD Biosciences, Bedford, MA) and following the manufacturer's instructions. The assay was also prepared as described in Kong et al.[10] The transepithelial electrical resistance (TEER) value of each Caco-2 cell monolayer integrity was measured using a Millicell-ERS Voltohmmeter (Millipore Corp., Bedford, MA), which was provided by Dr. M. Jung (Georgetown University, Washington, DC). A TEER of above 400 Ω/cm^2 was used for the transport assay. The transport of Lucifer yellow across the monolayer for 1 h was also determined for Caco-2 cell monolayer integrity evaluation by using wavelengths of 485 nm excitation and 535 nm emission of the fluorescence at the end of the transport experiments. Briefly, 100 μM of the test compound in HBSS buffer was added to either the apical or basolateral side of the Caco-2 cell monolayers, which were preincubated with prewarmed HBSS buffer (pH 7.4) at 37 °C, 5% CO_2, and 100% humidity for 10 min. The plate was incubated and shaken at 37 °C, 5% CO_2, 100% humidity, and 50 rpm for 2 h. Aliquots of 500 μL were taken from each receiver chamber and replaced with equal volumes of HBSS buffer at the predetermined time intervals. The concentration of test compound was analyzed by HPLC. As a standard compound, propranolol and atenolol were also evaluated.[11,12] For the data analysis, apparent permeability coefficients (P_{app}, cm/sec) were calculated by using the following equation as previously published:[10,13]

$$P_{app} = \frac{V}{AC_0} \frac{dQ}{dt}$$

where V is the volume (mL) in acceptor side, A is the membrane surface area (cm^2), and C_0 is the initial concentration of test compound in the donor side (nmol/mL). dQ/dt is the appearance rate of the test compound at the acceptor side (nmol/mL s).

Solubility and Chemical Stability. To measure solubility, VMY-2-95 (20 mg) or VMY-2-95·2HCl (50 mg) was shaken in 1 mL of pH 6.8 isotonic phosphate buffer solution for 24 h at 25 °C. A 50 μL portion of the supernatant was analyzed by HPLC after centrifugation. For chemical stability, a solution of VMY-2-95·2HCl (1 mM) was incubated in pH 1.2 hydrochloric acid buffer or pH 6.8 isotonic phosphate buffer at 37 °C for 24 h. At a predetermined time interval, the concentration of VMY-2-95·2HCl was analyzed by HPLC.

Apparent Partition Coefficient. The apparent partition coefficient of VMY-2-95·2HCl was measured according to published protocol.[10,14,15] Briefly, 10 mL of VMY-2-95·2HCl (1 mM) solution in pH 6.8 isotonic phosphate buffer presaturated with 1-octanol was shaken with 10 mL of 1-octanol presaturated with pH 6.8 isotonic phosphate buffer for 10 h and left for 6 h at 37 °C. The concentration of VMY-2-95·2HCl in the aqueous phase was determined by HPLC. The apparent partition coefficient was calculated by using the following equation: $\log P_{oct} = \log(C_0 - C_w)/C_w$, where C_0 is the initial concentration and C_w represent the equilibrium concentration of the compound in aqueous phase. $C_0 - C_w$ is the concentration in octanol phase.

Metabolic Human Liver Microsomes Assay. For this study, we prepared *in vitro* CYP H-class 10-donor mixed gender pooled human liver microsomes from Celsis In Vitro Technologies Inc. (Baltimore, MD) as previously published.[10,16,17] The reaction mixture was prepared with human liver microsomes (1 mg/mL), NADP$^+$ (1 mM), G-6-PDH (2U/mL), and glucose 6-phosphate (10 mM) in 100 mM PBS (pH 7.4) containing 10 mM $MgCl_2$. This mixture was preincubated and shaken at 37 °C, 5% CO_2, 100% humidity, and 50 rpm for 10 min. The reaction was initiated by the addition of VMY-2-95·2HCl (10 μM) or positive control, testosterone (10 μM), to the reaction mixture, incubated and shaken at the same conditions for 2 h. Aliquots of 200 μL were taken from the reaction mixture and added to 800 μL of ice-cold stop solution consisting of acetonitrile/methanol (50/50, v/v) at the predetermined time intervals. The concentration of VMY-2-95·2HCl was analyzed by HPLC. As a positive control for the human liver, microsome activity of testosterone was also evaluated.[16,18,19]

Inhibition of Cytochrome P450 (CYP450). The high throughput inhibition screening kits for human recombinant CYP450-selective enzymes were obtained from BD Biosciences (Bedford, MA). Each kit was for CYP1A2/CEC, CYP2C9/MFC, CYP2C19/CEC, CYP2D6/AMMC, or CYP3A4/BQ. The composition of the assay was summarized in a previously reported Table.[10] The assay was performed by following the manufacturer's instructions. Briefly, 10 mM VMY-2-95·2HCl (50 μL) and each positive control (50 μL) of selective enzymes in acetonitrile were prepared in a 96-well black microtiter plate and preincubated with NADPH-cofactor mixture (100 μL) at 37 °C for 10 min. The reaction was initiated by the addition of 100 μL of enzyme/substrate mixture and incubated at 37 °C for 15, 30, or 45 min, and 75 μL of cold stop reagent composed of acetonitrile/0.5 M Tris base (80/20, v/v) was added. The concentration of VMY-2-95·2HCl and positive control was determined by fluorescence measurement.

HPLC Analysis. The HPLC system consisted of LC-20AD pumps, a SDP-10AV UV detector, a DGU-20A degasser, a CBM-20A connector, and a SIL-HT$_A$ autosampler from Shimadzu Corporation. A Symmetry C18 column (4.6 × 250 mm, 5 μm) equipped with a C18 guard column from Waters Corporation was eluted with the mobile phase. The mobile phase consisted of acetonitrile/water containing 0.1% acetic acid (90/10, v/v) for VMY-2-95·2HCl, acetonitrile/water

containing 0.1% acetic acid (20/80, v/v) for propranolol, and acetonitrile/water containing 0.1% triethylamine (25/75, v/v) for atenolol. The UV absorbance was detected at 254 nm. The flow rate was 1.0 mL/min. The retention time of VMY-2-95·2HCl, propranolol, and atenolol was 5.48, 6.92, and 5.10 min, respectively. Standard curves were linear in the range of 0.01−1000 μg/mL of stock solutions of compounds (r^2 = 0.999).

Pharmacokinetics Studies. Six male Sprague−Dawley (SD) rats with weight 210 ± 15 g were supplied by Vital River Experimental Animal Ltd. (Beijing, China). The rats were housed under controlled conditions (temperature, 23 ± 1 °C; humidity, 55 ± 5%) with a commercial food diet and water freely available. Animal experiments were carried out according to institutional guidelines for the care and the use of laboratory animals and approved by the Animal Ethics Committee of Chinese Academy of Medical Sciences. The rats were acclimatized to the facilities for 7 days, and then fasted for 12 h and had free access to water before experiment. VMY-2-95·2HCl was suspended in water. Blood samples were collected predose and subsequently at 0.25, 0.5, 1, 2, 3, 4, 5, 7, 9, 12, and 24 h after i.g. administration of VMY-2-95·2HCl (75 mg/kg). The blood samples were centrifuged at 5000 rpm for 10 min at 4 °C. Then 180 μL of plasma was transferred to another tube and stored at −20 °C until analysis; 180 μL volume of blank plasma, calibration standards, or plasma samples were spiked into 18 μL of carbamazepine (10 μg/mL, IS) and 800 μL of ethyl acetate. After vortexing for 3 min and centrifuging at 13,400 rpm for 10 min at 4 °C, the organic layer was transferred immediately to another tube and dried under N$_2$. The residue was reconstituted with 90 μL of mobile phase and 30 μL was injected into HPLC system for analysis. Chromatography analysis was performed with Agilent HPLC 1200 system (Agilent, USA). The chromatographic separation was carried out using an Agilent Zorbax SB-C18 column (4.6 × 250 mm, 5 μm) with a guard column (Agilent Zorbax SB-C18 Column, 4.6 × 12.5 mm, 5 μm). The column temperature was maintained at 30 °C. The mobile phase consisted of 0.1% phosphoric acid and acetonitrile (v/v) using a gradient elution below: 0.0−10.0 min, 25% acetonitrile → 34% acetonitrile; 10.0−16.0 min, 34% acetonitrile; 16.0 min, 25% acetonitrile. The flow rate was 1 mL/min and the wavelength was set at 282 nm. Under the assay conditions, no endogenous interference was observed and the retention time of VMY-2-95·2HCl and internal standard (IS) were 6.8 and 15.2 min, respectively. The calculated peak area ratios of VMY-2-95·2HCl to the IS (R) versus the nominal concentration (C) displayed a good linear relationship ranging from 0.0977−25 μg/mL. The regression equation was R = 0.7875C − 0.1464 (R^2 = 0.9993, n = 5). Intra- and inter-run precision, accuracy, and recovery at concentrations of 0.78125, 3.125, and 12.5 μg/mL are provided in Supporting Information Table 1.

Determination of VMY-2-95·2HCl in the SD Rat Brain and the Plasma after Oral Administration. Male SD rats were prepared and maintained using the protocol approved by the Georgetown University Animal Welfare Committee (#11−029) and the Animal Care guidelines. These animals were fasted for 12 h prior to the administration of VMY-2-95·2HCl. VMY-2-95·2HCl (3 mg/kg) in 0.3 mL of water was administered to rats by a gastric intubation. After 30 min, 1 h, or 3 h, the animals were sacrificed and the whole brain and the blood were collected separately. The brain tissue was immediately homogenized in cold pH 7.4 PBS and stored at −80 °C until analyzed by mass spectrometry (MS). The plasma

was immediately removed from blood samples after centrifugation for 5 min at 14,000 rpm at 4 °C and stored at −80 °C until analysis by MS. A standard curve was made by spiking the internal standard (E2, C$_{31}$H$_{29}$N$_3$O$_5$, m/z = 524.37, Supporting Information Figure 1) at final concentrations of 0.062 and 0.16 μg/mL of VMY-2-95 and making serial dilutions to obtain a seven point concentration range of 0.001 to 0.16 μg/mL.

Sample quantitation of VMY-2-95 was performed using multiple reaction monitoring mass spectrometry. The samples were resolved on an Acquity UPLC BEH C18 1.7 μm, 2.1 × 100 mm column online with a triple quadrupole mass spectrometer (Xevo-TQ, Waters Corporation, USA) operating in the multiple reaction monitoring (MRM) mode. The sample cone voltage and collision energies were optimized for VMY-2-95 to obtain maximum ion intensity for parent and daughter ions using "IntelliStart" feature of MassLynx software (Waters Corporation, USA). The instrument parameters were optimized to gain maximum specificity and sensitivity of ionization for the parent [m/z = 265.1] and daughter ions. Signal intensities from all MRM Q1/Q3 ion pairs for VMY-2-95 were ranked to ensure selection of the most intense precursor and fragment ion pair for MRM-based quantitation. This approach resulted in selection of cone voltages and collision energies that maximized the generation of each fragment ion species; the MRM parameters are specified in Supporting Information Figure 1. The metabolite ratios were calculated by normalizing the peak area of endogenous metabolites within tissue samples normalized to the internal standard. Since a stable isotope labeled standard of the drug was not available, we used another compound, E2 (C$_{31}$H$_{29}$N$_3$O$_5$, m/z = 524.37, Supporting Information Figure 1), synthesized in the laboratory and similar in structure and chromatographic retention time for this purpose. The sample queue was randomized, and solvent blanks were injected to assess sample carryover. To determine the inter assay reproducibility of the MRM experiments, two independent analyses were performed with a six point calibration curve.

Acute Toxicity Methods. The single-dose acute toxicity of VMY-2-95·2HCl was measured in female SD rats according to CHAMPIX (Varenicline, Pfizer) method[20−22] and modified with the protocol, the acute oral toxicity (AOT) up and down procedure.[23] Female SD rats were purchased from the National Cancer Institute (NCI). The animal protocol was approved by the Georgetown University Animal Welfare Committee and followed to the Animal Care guidelines. VMY-2-95·2HCl stock solution was prepared in water and the concentration was 200 mg/mL. VMY-2-95·2HCl (100, 200, 300, and 400 mg/kg) was administered orally, and uninterrupted observations were maintained for the first 4 h. The acute toxicity was observed daily for 14 days. Animals were sacrificed and all pathological findings were recorded.

■ RESULTS

Solubility, pH Stability, and Apparent Partition Coefficient. The chemical structure for VMY-2-95 is shown in Figure 1A. The solubility of VMY-2-95 was found to be 0.604 mg/mL in pH 6.8 isotonic phosphate buffer at 25 °C and freely soluble in DMSO. To improve the solubility of VMY-2-95, the HCl salt of VMY-2-95 (VMY-2-95·2HCl) was prepared and studied. VMY-2-95·2HCl solubility in buffer was more than 50 mg/mL. To examine whether VMY-2-95·2HCl would be chemically stable during passing the gastrointestinal tract or in the system, VMY-2-95·2HCl was incubated in pH 1.2 or 6.8

buffer solution at 37 °C for 24 h, where a pH 1.2 buffer solution represents gastric acid and pH 6.8 does intestinal fluids. VMY-2-95·2HCl was stable, showing no change in 1 mM of VMY-2-95·2HCl or production of any new chemical entities during the incubation period (Figure 2A). The log scale of apparent partition coefficient of VMY-2-95·2HCl in 1-octanol/phosphate-buffered (pH 6.8) solution was 0.682 at 37 °C.
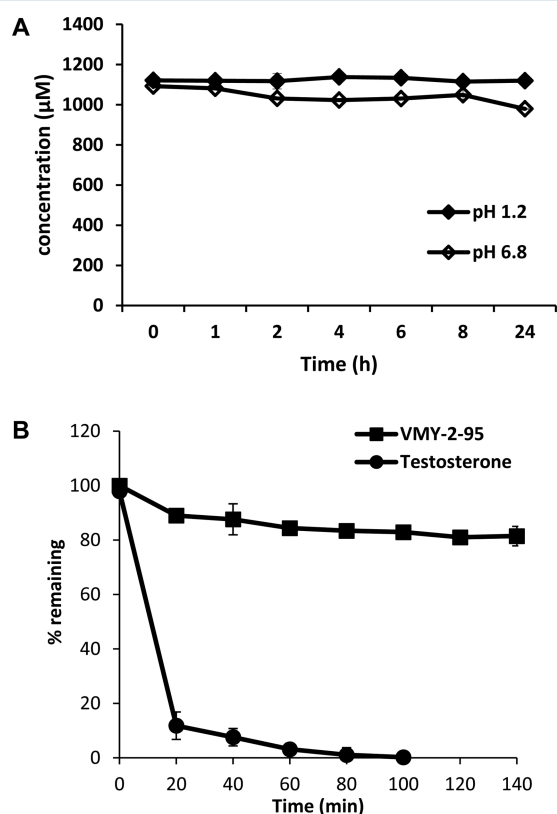

Figure 2. (A) Chemical stability of VMY-2-95·2HCl in pH 1.2 hydrochloric acid buffer or pH 6.8 isotonic phosphate buffer at 37 °C for 24 h. (B) Incubation of 10 μM VMY-2-95·2HCl or 10 μM testosterone in 10-donor mixed gender pooled human liver microsomes (1 mg/mL) for 2 h. The concentration of VMY-2-95·2HCl was analyzed by HPLC. Data are mean ± SD ($n = 3$).

Metabolic Stability in Human Liver Microsomes. The *in vitro* Phase-I metabolic stability of VMY-2-95·2HCl was determined in 10-donor mixed gender pooled human liver microsomes with the cofactors by monitoring the disappearance of the parent compound over an incubation period of 2 h. As seen in Figure 2B, 10 μM VMY-2-95·2HCl was shown slight decrease of only about 19% over the 2 h period in the presence of human liver microsomes. No new UV-active chemical entities were detected by HPLC. For the positive compound of human liver microsomes activity, the stability of 10 μM testosterone was evaluated,[16,17] showing that more than 95% of parent compound disappeared rapidly over the 2 h incubation period (Figure 2B).

Inhibition of Cytochrome P450. VMY-2-95·2HCl was incubated with human recombinant CYP450-selective enzymes CYP1A2, 2C9, 2C19, 2D6, and 3A4. In Figure 3, the dose–response curves were demonstrated for VMY-2-95·2HCl and each control compound. IC$_{50}$ value for the effect of VMY-2-95·2HCl on each enzyme is shown in Table 1. VMY-2-95·2HCl was evaluated in a dose-dependent manner on the metabolism

mediated by CYP1A2, 2C9, 2C19, 2D6, and 3A4. VMY-2-95·2HCl exhibited IC$_{50}$ values of 10.64, 5.11, and 1.12 μM against CYP1A2, CYP2C9, and 2C19, respectively. VMY-2-95·2HCl showed weak inhibition of CYP3A4 activity with an IC$_{50}$ value of 9.73 μM and no inhibitor activity on 2D6 was exhibited. The reference compounds, furafylline, sulfaphenazole, tranylcypromine, quinidine, and ketoconazole for CYP1A2, 2C9, 2C19, 2D6, and 3A4, respectively, showed IC$_{50}$ values of 6.33, 0.29, 0.68, 0.002, and 0.01 μM, respectively.

Transport Studies of VMY-2-95·2HCl. In vitro transport and permeability model using human colonic adenocarcinoma Caco-2 cells is a widely used method to predict the intestinal absorption and bioavailability of drug.[16,24] To make a fast, efficient, and ready-to-use Caco-2 cell monolayer model, Uchida et al. reported a modified Caco-2 permeability assay system, which takes only 3 to 5 days.[24] We used a 4 day-system on collagen-coated inserts for Caco-2 cell monolayer as described in the Materials and Methods. The tightness of Caco-2 cell monolayer was assessed by determining the TEER values and % passage of Lucifer yellow. The time–concentration profiles of VMY-2-95·2HCl showed the bilateral permeation kinetics in Figure 4. The permeation rates in both apical to basolateral (Figure 4A) and basolateral to apical (Figure 4B) directions increased dose-dependently, while the apparent permeability coefficient (P_{app}) values remained unchanged with 100 μM concentrations of VMY-2-95·2HCl (Table 2). VMY-2-95·2HCl exhibited linear transport across the Caco-2 cell monolayer over a 2 h period. Table 2 summarizes the P_{app} values for the permeation of the compounds across Caco-2 cell monolayers in both directions. VMY-2-95·2HCl exhibited P_{app} value of 21.1 × 10^{-6} cm/sec (100 μM) in apical to basolateral direction, and P_{app} value of VMY-2-95·2HCl for basolateral to apical direction was 23.4 × 10^{-6} cm/sec (100 μM). VMY-2-95·2HCl at a concentration of 100 μM was found to have efflux ratio values of 1.11 by employing P_{app}B−A/P_{app}A−B. The well-known paracellular transport marker, atenolol,[12] and passive transcellular transport marker, propranolol,[11] were examined for low and high permeability, respectively, in Caco-2 cell monolayers. P-gp, MRP1, and MRP2 are well-known efflux transporters, which are located on the apical side and MRP2 on the basolateral side of Caco-2 cell monolayers and mediated the efflux of a variety of xenobiotics, resulting in limitation of absorption and elimination of drug.[25] To investigate whether the transport of VMY-2-95·2HCl is mediated by P-gp and MRP1/MRP2, a P-gp inhibitor, verapamil, or MRP1/MRP2 inhibitor, MK-571,[26] was preincubated in Caco-2 cell monolayers. The efflux ratio of both VMY-2-95·2HCl with verapamil and VMY-2-95·2HCl with MK-571 was about 1 (Table 2). These results show that VMY-2-95·2HCl might have good permeability through the gastrointestinal tract without being affected by P-gp or MRP1/MRP2.

Pharmacokinetic Study of VMY-2-95·2HCl. The time–concentration profile of VMY-2-95·2HCl in plasma after oral administration to rats is shown in Figure 5. VMY-2-95·2HCl achieved a plasma half-life of 8.98 h after oral administration and showed that the C_{max} was 0.56 μg/mL at 0.9 h and the AUC was 7.05 μg/h·mL. We summarized the pharmacokinetic data of VMY-2-95·2HCl in Table 3, and the data suggest that VMY-2-95·2HCl has sufficient *in vivo* absorption following oral administration.

Measurement of VMY-2-95·2HCl in the Brain Tissue and the Plasma after Oral Administration. For *in vivo*
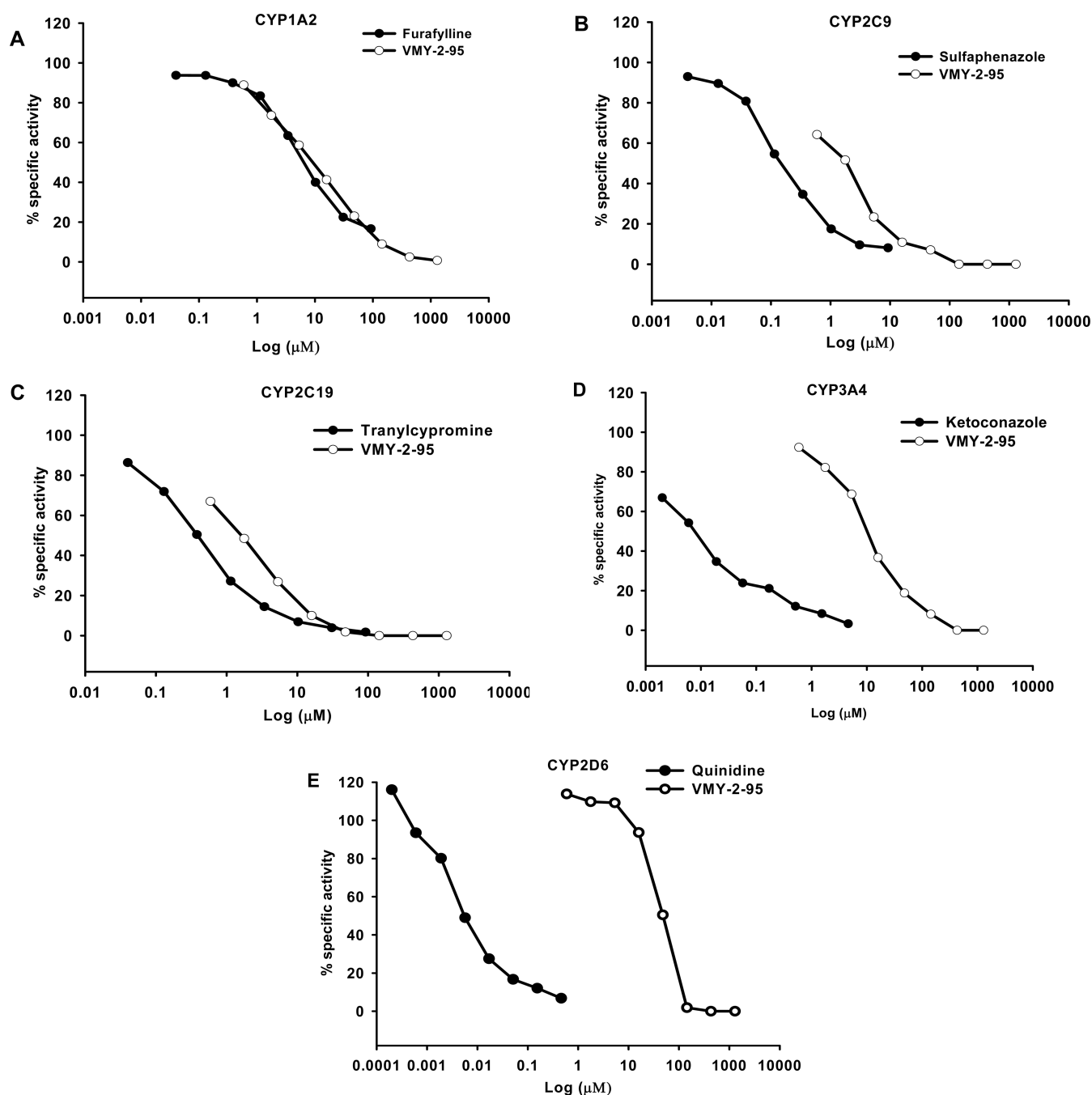
Figure 3. Inhibition of CYP450 activity of VMY-2-95·2HCl and reference compounds is shown in a dose range from 0.001 to 10,000 μM (logarithmic scale). (A) Percent specific activity of VMY-2-95·2HCl and furafylline on CYP1A2. (B) Percent specific activity of VMY-2-95·2HCl and sulfaphenazole on CYP2C9. (C) Percent specific activity of VMY-2-95·2HCl and tranylcypromine on CYP2C19. (D) Percent specific activity of VMY-2-95·2HCl and ketochonazole on CYP3A4. (E) Percent specific activity of VMY-2-95·2HCl and quinidine on CYP2D6. The mean of duplicate analysis is shown.

efficacy, VMY-2-95·2HCl should not only exhibit biostability but should also achieve significant brain levels. VMY-2-95·2HCl was administered orally to rats, and the brain tissue and plasma concentration of the compound were determined. As shown in Figure 6A, VMY-2-95·2HCl was rapidly absorbed and the maximal brain tissue concentration reached about 2.3 μg/g within 60 min. Plasma levels were also measured to examine the systemic absorption of VMY-2-95·2HCl during the transition to the brain (Figure 6B). While oral administration of VMY-2-95·2HCl led to rapid absorption in the brain, the plasma concentration of VMY-2-95·2HCl after oral administration

was low and the maximal plasma concentration achieved 0.05 μg/mL. This result suggests that VMY-2-95·2HCl is efficiently delivered to the brain tissue.

Acute Toxicity Study. The acute toxicity of VMY-2-95·2HCl was measured *in vivo* in female SD rats by oral administration. No toxicity (including no change in body weight) and mortality were observed during 14 days of monitoring after oral administration of 100, 200, 300, or 400 mg/kg.

Table 1. IC$_{50}$ Values (μM) of VMY-2-95 and Reference Compounds on CYP1A2, CYP2C9, CYP2C19, CYP2D6, and CYP3A4 High Throughput Inhibition Screening[a]

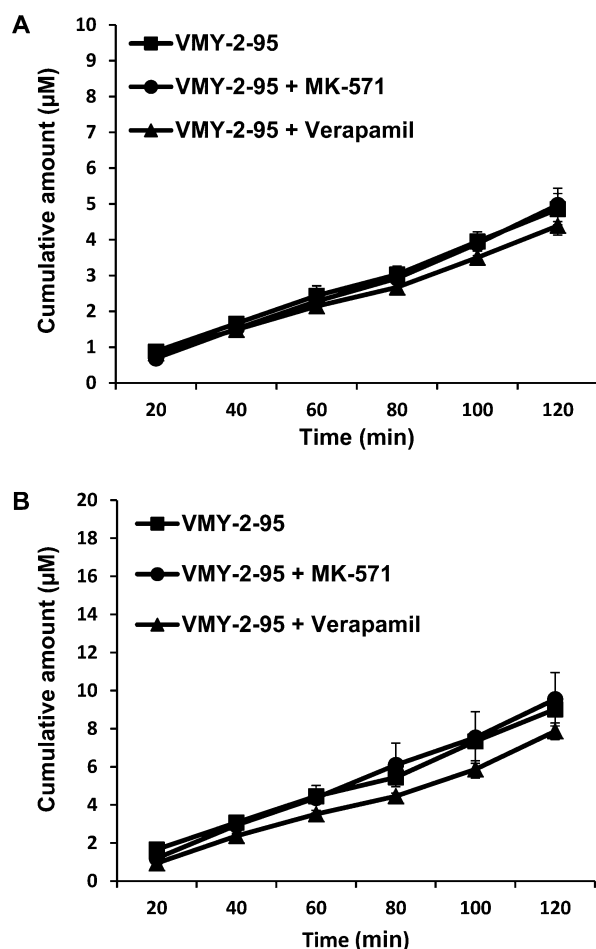| compound	enzyme				
	CYP1A2	CYP2C9	CYP2C19	CYP2D6	CYP3A4
VMY-2-95·2HCl	10.64 ± 0.004	5.11 ± 0.004	1.12 ± 0.006	142.68 ± 0.004	9.73 ± 0.002
furafylline	6.33 ± 0.007	NT	NT	NT	NT
sulfaphenazole	NT	0.29 ± 0.001	NT	NT	NT
tranylcypromine	NT	NT	0.68 ± 0.008	NT	NT
quinidine	NT	NT	NT	0.002 ± 0.000	NT
ketoconazole	NT	NT	NT	NT	0.01 ± 0.006

[a]NT = not tested.

Figure 4. (A) Cumulative amount of VMY-2-95·2HCl or with MK-571 or verapamil in apical to basolateral direction transported across Caco-2 cell monolayers. (B) Cumulative amount of VMY-2-95·2HCl or with MK-571 or verapamil in basolateral to apical direction transported across Caco-2 cell monolayers. The concentration of VMY-2-95·2HCl was analyzed by HPLC. Data are mean ± SD (n = 3).

DISCUSSION

Although potency and receptor selectivity are important to efficacy and safety, absorption, distribution, metabolism, and excretion (ADME) properties are vital factors for consideration of a new drug candidate. Critical molecular properties required for adequate delivery of an orally administered drug to the target site include solubility, lipophilicity, stability, and permeability. In long-term drug administration, imbalances in these properties can lead to serious side effects as a result of

Table 2. Permeability (P_{app}) of VMY-2-95 Across Caco-2 Cell Monolayers.[a]

compound (concentration)	drug transport P_{app} (× 10^{-6} cm/sec)		efflux ratio
	A → B	B → A	
VMY-2-95·2HCl (100 μM)	21.1 ± 0.02	23.4 ± 0.02	1.11
VMY-2-95·2HCl (100 μM) + verapamil (100 μM)	20.2 ± 0.02	20.7 ± 0.02	1.02
VMY-2-95·2HCl (100 μM) + MK-571 (100 μM)	23.0 ± 0.27	26.9 ± 0.32	1.17

[a]Bidirectional transport of VMY-2-95 was observed across Caco-2 cell monolayers for 2 h in the absence and presence of 100 μM P-gp inhibitor, verapamil, or 100 μM MRP1/MRP2 inhibitor, MK-571. Data are mean ± SD (n = 3). Efflux ratio = P_{app}B–A/P_{app}A–B.
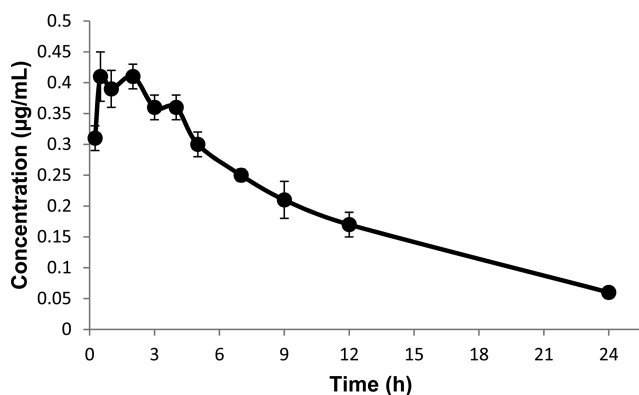

Figure 5. Plasma concentration of VMY-2-95·2HCl after oral administration in SD rats: 75 mg/kg VMY-2-95·2HCl suspension was prepared in water and administered orally to rats (210 ± 15 g). At an appropriate time interval, blood was collected and the concentration of VMY-2-95·2HCl in the plasma was determined by HPLC. Data are mean ± SD (n = 6).

Table 3. Pharmacokinetic Properties of VMY-2-95 in Plasma after Oral Administration to SD Rats[a]

parameter	VMY-2-95·2HCl
C_{max} (μg/mL)	0.56 ± 0.02
T_{max} (h)	0.92 ± 0.59
$T_{1/2}$ (h)	8.98 ± 2.36
AUC$_{0-last}$ (μg/mL·h)	7.05 ± 1.61
MRT (h)	8.03 ± 2.36

[a]AUC, area under the curve; MRT, mean residence time.

impeded elimination, toxic metabolites, and/or increased drug dose. In this study, we investigated physicochemical properties and oral bioavailability of VMY-2-95·2HCl.
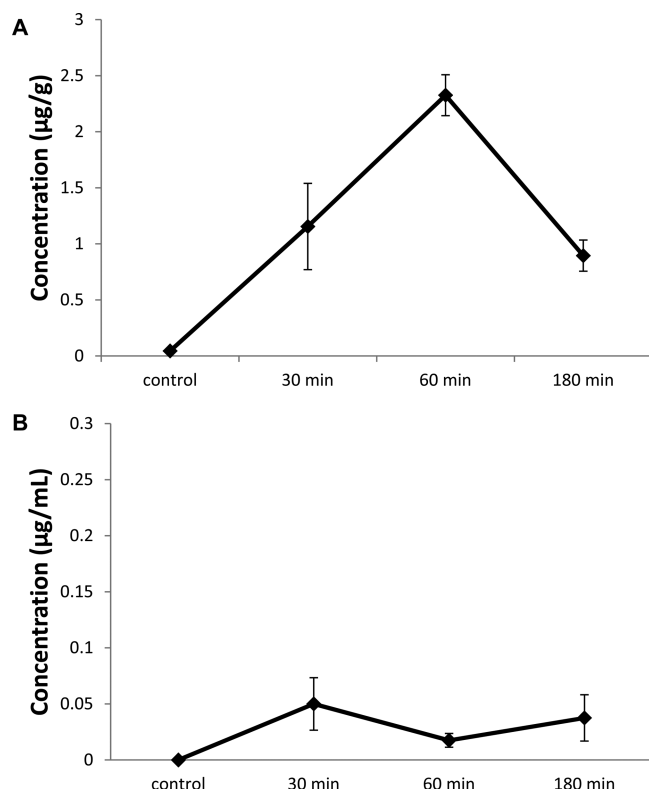
Figure 6. Brain and plasma concentration of VMY-2-95·2HCl after oral administration in SD rats. Three mg/kg VMY-2-95·2HCl suspension was prepared in water and administered orally to rats (210 ± 15 g). Control is the water treated group. At an appropriate time interval, brain tissue (A) and blood samples (B) were collected and the concentration of VMY-2-95·2HCl in homogenized brain tissue (A) and the plasma (B) was determined by LCMS. Data are mean ± SD (n = 3).

Lipophilicity, often expressed as partition coefficient (log P_{oct}) in octanol/water, is an important physicochemical parameter influencing processes such as oral absorption, cellular uptake, and other pharmacokinetic properties. The n-octanol/ water partition coefficient is the predictor of drug absorption that describes the ability of a drug to partition into the lipophilic phase (octanol), which is comparable to a cell membrane.[27] Usually log P_{oct} values of drugs between 2 to 5 are predictive of good oral absorption in humans.[27,28] Compounds with increasing log P_{oct} values can result in increased oral absorption, plasma protein binding, and volume of distribution.[29] However, more lipophilic compounds also become more susceptible to CYP450 metabolism, leading to higher drug clearance.[30] The calculated lipophilicity of VMY-2-95 is 3.712. However, the solubility of VMY-2-95 in pH 6.8 isotonic phosphate buffer at 25 °C is 0.604 mg/mL. Because of very low solubility of the nonsalt form of VMY-2-95 in the aqueous phase, a log P_{oct} could not be measured. Altogether the chemical stability, highly solubility in buffer, and a log P_{oct} value of 0.682, suggest that VMY-2-95·2HCl may have good stability and GI absorption.

Permeability in vivo is a complex system including passive diffusion, paracellular, active transport, and efflux.[31,33,34] Caco-2 cell permeability is a well-developed in vitro strategy for prediction of drug transport, and monolayers contain tight junctions, microvilli, small intestinal enzymes, and efflux carrier proteins.[16] These efflux proteins contain P-gp and MRP family,

which mediate drug transport and chemotherapy resistance.[26,32−34] VMY-2-95·2HCl demonstrated highly permeable to Caco-2 cell monolayers both in the apical to basolateral direction and in the basolateral to apical direction. The transport of VMY-2-95·2HCl was not involved in P-gp or MRP. VMY-2-95·2HCl demonstrated sufficient in vivo absorption following oral administration.

Cytochrome P450s are the principal enzymes in the phase-I metabolism of almost all the clinically used drugs.[35] The inhibition of a CYP can result in failed clinical trials[31] resulting from serious drug side effects related to reduced intestinal absorption or increased clearance.[35] VMY-2-95·2HCl exhibited only a 19% decrease in 10-donor mixed gender pooled human liver microsomes but had a significant inhibitory effect on CYP1A2, CYP2C9, and CYP2C19, and a weak inhibitory effect on CYP3A4. These in vitro studies suggest that VMY-2-95· 2HCl may have a significant effect on the pharmacology of CYP1A2, CYP2C9, and CYP2C19.

Finally, we measured in vivo acute toxicity and pharmacokinetics of VMY-2-95·2HCl in rats. No toxicity was observed for VMY-2-95·2HCl with oral administration up to 400 mg/kg. Pharmacokinetic study in rats after oral administration resulted in detection of VMY-2-95·2HCl in the blood by HPLC, and a favorable C_{max}, $T_{1/2}$, and AUC were determined. Although the low partition coefficient of VMY-2-95·2HCl suggested that partitioning of the blood−brain barrier would be limited, however, VMY-2-95·2HCl was rapidly absorbed and efficiently achieved maximal brain levels (2.3 μg/g) by 1 h. High brain levels of VMY-2-95·2HCl detected at a maximum of 60 min provides evidence of significant brain exposure and provides support to observed efficacy in nicotine self-administration.[9] Taken together, our data suggest that VMY-2-95·2HCl has a promising oral bioavailability, acceptable pharmacokinetic properties, and significant brain exposure levels.

■ CONCLUSIONS

In conclusion, the present study demonstrates that VMY-2-95· 2HCl has good oral bioavailability without toxicity. VMY-2-95· 2HCl displays significant intestinal transport in the Caco-2 cell model predicting complete absorption in the gastrointestinal tract. VMY-2-95·2HCl is delivered to the brain and therapeutic concentrations of drug can be achieved. These studies support the use of VMY-2-95·2HCl in other preclinical studies to evaluate antidepressant, smoking cessation, or in models of drug addiction where CNS delivery is required.

■ ASSOCIATED CONTENT

ⓢ Supporting Information

Supporting tables and spectra. This material is available free of charge via the Internet at http://pubs.acs.org.

■ AUTHOR INFORMATION

Corresponding Author

*Tel: 202-687-8605. E-mail: mb544@georgetown.edu.

Author Contributions

⊥H.K. and J.-k.S contributed equally.

Notes

The authors declare the following competing financial interest(s): A patent application has been filed by Georgetown University on the behalf of the inventors that are listed as authors in this article.

ACKNOWLEDGMENTS

ABBREVIATIONS

TEER, transepithelial electrical resistance; MRP, multidrug resistance-associated protein; P-gp, P-glycoprotein; CYP450, cytochrome P450; AUC, area under the curve; MRT, mean residence time; MS, mass spectrometry; MRM, multiple reaction monitoring

REFERENCES

(1) CDC. Smoking-attributable morbidity, Years of potential life lost, and Productivity losses-United States, 2000−2004. Morbidity and Mortality Weekly Report CDC Department of health and human services; 2008; Vol. 57, Issue 45, pp 1226−8.

(2) Karlin, A. Emerging structure of the nicotinic acetylcholine receptors. *Nat. Rev. Neurosci.* 2002, 3 (2), 102−14.

(3) Millar, N. S. Assembly and subunit diversity of nicotinic acetylcholine receptors. *Biochem. Soc. Trans.* 2003, 31 (Pt 4), 869−74.

(4) Flores, C. M.; Rogers, S. W.; Pabreza, L. A.; Wolfe, B. B.; Kellar, K. J. A subtype of nicotinic cholinergic receptor in rat brain is composed of alpha 4 and beta 2 subunits and is up-regulated by chronic nicotine treatment. *Mol. Pharmacol.* 1992, 41 (1), 31−7.

(5) Marubio, L. M.; Gardier, A. M.; Durier, S.; David, D.; Klink, R.; Arroyo-Jimenez, M. M.; et al. Effects of nicotine in the dopaminergic system of mice lacking the alpha4 subunit of neuronal nicotinic acetylcholine receptors. *Eur. J. Neurosci.* 2003, 17 (7), 1329−37.

(6) Maskos, U.; Molles, B. E.; Pons, S.; Besson, M.; Guiard, B. P.; Guilloux, J. P.; et al. Nicotine reinforcement and cognition restored by targeted expression of nicotinic receptors. *Nature* 2005, 436 (7047), 103−7.

(7) Picciotto, M. R.; Zoli, M.; Rimondini, R.; Lena, C.; Marubio, L. M.; Pich, E. M.; et al. Acetylcholine receptors containing the beta2 subunit are involved in the reinforcing properties of nicotine. *Nature* 1998, 391 (6663), 173−7.

(8) Tapper, A. R.; McKinney, S. L.; Nashmi, R.; Schwarz, J.; Deshpande, P.; Labarca, C.; et al. Nicotine activation of alpha4* receptors: sufficient for reward, tolerance, and sensitization. *Science* 2004, 306 (5698), 1029−32.

(9) Venkata, M.; Yenugonda, Y. X.; Levin, E. D.; Rezvani, A. H.; Tran, T.; Al-Muhtasib, N.; Sahizzada, N.; Xie, T.; Wells, C.; Slade, S.; Johnson, J. E.; Dakshanamurthy, S.; Kong, H.; Tomita, Y.; Liu, Y.; Paige, M.; Kellar, K. J.; Brown, M. L. Design, synthesis and discovery of picomolar selective α4β2 nicotinic acetylcholine receptor ligands. *J. Med. Chem.* 2013, 56 (21), 8404−21.

(10) Kong, H. S.; Tian, S.; Kong, Y.; Du, G.; Zhang, L.; Jung, M.; et al. Preclinical studies of YK-4−272, an inhibitor of class II histone deacetylases by disruption of nucleocytoplasmic shuttling. *Pharm. Res.* 2012, 29 (12), 3373−83.

(11) Frederick, K. S.; Maurer, T. S.; Kalgutkar, A. S.; Royer, L. J.; Francone, O. L.; Winter, S. M.; et al. Pharmacokinetics, disposition and lipid-modulating activity of 5-{2-[4-(3,4-difluorophenoxy)-phenyl]-ethylsulfamoyl}-2-methyl-benzoic acid, a potent and subtype-selective peroxisome proliferator-activated receptor alpha agonist in preclinical species and human. *Xenobiotica* 2009, 39 (10), 766−81.

(12) Bey, E.; Marchais-Oberwinkler, S.; Werth, R.; Negri, M.; Al-Soud, Y. A.; Kruchten, P.; et al. Design, synthesis, biological evaluation and pharmacokinetics of bis(hydroxyphenyl) substituted azoles, thiophenes, benzenes, and aza-benzenes as potent and selective nonsteroidal inhibitors of 17beta-hydroxysteroid dehydrogenase type 1 (17beta-HSD1). *J. Med. Chem.* 2008, 51 (21), 6725−39.

(13) Artursson, P.; Karlsson, J. Correlation between oral drug absorption in humans and apparent drug permeability coefficients in human intestinal epithelial (Caco-2) cells. *Biochem. Biophys. Res. Commun.* 1991, 175 (3), 880−5.

(14) Doh, M. J.; Jung, Y. J.; Kim, I.; Kong, H. S.; Kim, Y. M. Synthesis and in vitro properties of prednisolone 21-sulfate sodium as a colon-specific prodrug of prednisolone. *Arch. Pharm. Rese.* 2003, 26 (4), 258−63.

(15) Lee, J.; Rho, J.; Yang, Y.; Kong, H.; Jung, Y.; Kim, Y. Synthesis and in vitro evaluation of N-nicotinoylglycyl-2-(5-fluorouracil-1-yl)-D,L-glycine as a colon-specific prodrug of 5-fluorouracil. *J. Drug Targeting* 2007, 15 (3), 199−205.

(16) Madgula, V. L.; Avula, B.; Pawar, R. S.; Shukla, Y. J.; Khan, I. A.; Walker, L. A.; et al. In vitro metabolic stability and intestinal transport of P57AS3 (P57) from Hoodia gordonii and its interaction with drug metabolizing enzymes. *Planta Medica* 2008, 74 (10), 1269−75.

(17) Obach, R. S.; Baxter, J. G.; Liston, T. E.; Silber, B. M.; Jones, B. C.; MacIntyre, F.; et al. The prediction of human pharmacokinetic parameters from preclinical and in vitro metabolism data. *J. Pharmacol. Exp. Ther.* 1997, 283 (1), 46−58.

(18) Obach, R. S. Prediction of human clearance of twenty-nine drugs from hepatic microsomal intrinsic clearance data: An examination of in vitro half-life approach and nonspecific binding to microsomes. *Drug Metab. Dispos.* 1999, 27 (11), 1350−9.

(19) Obach, R. S. The prediction of human clearance from hepatic microsomal metabolism data. *Curr. Opin. Drug Discovery Dev.* 2001, 4 (1), 36−44.

(20) (EMEA) TEMEA. Champix, INN-Varenicline tartrate. 2006; pp 1−44.

(21) Obach, R. S.; Reed-Hagen, A. E.; Krueger, S. S.; Obach, B. J.; O'Connell, T. N.; Zandi, K. S.; et al. Metabolism and disposition of varenicline, a selective alpha4beta2 acetylcholine receptor partial agonist, in vivo and in vitro. *Drug Metab. Dispos.* 2006, 34 (1), 121−30.

(22) Jimenez-Ruiz, C.; Berlin, I.; Hering, T. Varenicline: a novel pharmacotherapy for smoking cessation. *Drugs* 2009, 69 (10), 1319−38.

(23) OECD. Acute oral toxicity-up and down procedure. OECD Guides for testing of chemicals. 2001.

(24) Uchida, M.; Fukazawa, T.; Yamazaki, Y.; Hashimoto, H.; Miyamoto, Y. A modified fast (4 day) 96-well plate Caco-2 permeability assay. *J. Pharmacol. Toxicol. Methods* 2009, 59 (1), 39−43.

(25) Hirohashi, T.; Suzuki, H.; Chu, X. Y.; Tamai, I; Tsuji, A.; Sugiyama, Y. Function and expression of multidrug resistance-associated protein family in human colon adenocarcinoma cells (Caco-2). *J. Pharmacol. Exp. Ther.* 2000, 292 (1), 265−270.

(26) Sambuy, I.; De Angelis, I.; Ranaldi, G.; Scarino, M. L.; Stammati, A.; Zucco, F. The Caco-2 cell line as a model of the intestinal barrier: influence of cell and culture-related factors on Caco-2 cell functional characteristics. *Cell Biol. Toxicol.* 2005, 21 (1), 1−26.

(27) Artursson, P.; Palm, K.; Luthman, K. Caco-2 monolayers in experimental and theoretical predictions of drug transport. *Adv. Drug Delivery Rev.* 2001, 46 (1−3), 27−43.

(28) Wils, P.; Warnery, A.; Phung-Ba, V.; Legrain, S.; Scherman, D. High lipophilicity decreases drug transport across intestinal epithelial cells. *J. Pharmacol. Exp. Ther.* 1994, 269 (2), 654−8.

(29) Stewart, B. H.; Chan, O. H.; Lu, R. H.; Reyner, E. L.; Schmid, H. L.; Hamilton, H. W.; et al. Comparison of intestinal permeabilities determined in multiple in vitro and in situ models: relationship to absorption in humans. *Pharm. Res.* 1995, 12 (5), 693−9.

(30) Alavijeh, M. S.; Chishty, M.; Qaiser, M. Z.; Palmer, A. M. Drug metabolism and pharmacokinetics, the blood-brain barrier, and central nervous system drug discovery. *NeuroRx* 2005, 2 (4), 554−71.

(31) Kerns, E. H.; Kleintop, T.; Little, D.; Tobien, T.; Mallis, L.; Di, L.; et al. Integrated high capacity solid phase extraction-MS/MS system for pharmaceutical profiling in drug discovery. *J. Pharm. Biomed. Anal.* 2004, 34 (1), 1−9.

(32) Konsoula, Z.; Jung, M. Involvement of P-glycoprotein and multidrug resistance associated protein 1 on the transepithelial transport of a mercaptoacetamide-based histone-deacetylase inhibitor in Caco-2 cells. *Biol. Pharm. Bull.* 2009, 32 (1), 74−8.

(33) Wang, Q.; Rager, J. D.; Weinstein, K.; Kardos, P. S.; Dobson, G. L.; Li, J.; et al. Evaluation of the MDR-MDCK cell line as a

permeability screen for the blood-brain barrier. *Int. J. Pharm.* **2005**, *288* (2), 349−59.

(34) Madgula, V. L.; Avula, B.; Reddy, V. L. N.; Khan, I. A.; Khan, S. I. Transport of decursin and decursinol angelate across Caco-2 and MDR-MDCK cell monolayers: in vitro models for intestinal and blood-brain barrier permeability. *Planta Medica* **2007**, *73* (4), 330−5.

(35) Crespi, C. L.; Penman, B. W. Use of cDNA-expressed human cytochrome P450 enzymes to study potential drug-drug interactions. *Adv. Pharmacol.* **1997**, *43*, 171−88.